Letters

Reconfigurable LLC Topology With Squeezed Frequency Span for High-Voltage Bus-Based Photovoltaic Systems

Ming Shang, Haoyu Wang, and Qi Cao

***Abstract*—In high-voltage bus-based photovoltaic systems, an isolated dc/dc converter is required to link the wide range low-voltage solar panel and the high-voltage dc bus. In this letter, a novel LLC topology with reconfigurable voltage multiplier rectifier is proposed for use in such applications. Depending on different input voltages, its rectifier automatically switches among type-4, type-5, and type-6 voltage multiplier configurations. Thus, the switching frequency range can be effectively squeezed and the efficiency over wide input range can be enhanced. Zero voltage switching and zero current switching are realized among all power MOSFETs and all power diodes, respectively. A 300 W prototype converting a 25–50 V input to a 760 V bus is designed and tested both in steady state and dynamically. Both the circuit functionality and the theoretical analysis are verified by the experimental results. The prototype demonstrates 96.1% peak efficiency and good overall efficiency performance over a wide input range.**

***Index Terms*—LLC topology, microinverter, reconfigurable voltage multiplier rectifier, zero voltage switching (ZVS).**

I. Introduction

TYPICALLY, a two-stage microinverter includes (a) the front-end isolated dc/dc converter to step up the photovoltaic (PV) panel voltage to the dc bus, and (b) the second stage inverter to convert the dc bus to the utility grid [1], [2]. In the second stage, a half-bridge inverter with 760 V dc bus is considered as a good candidate [3]. This is because the half-bridge inverter is featured with reduced components count, enhanced power density, and improved circuit reliability. Fig. 1 demonstrates the block diagram of such a 760 V bus-based two-stage microinverter. Generally, the power level of microinverters is within 100–300 W [4], [5], and the output voltage of the PV panel is lower than 50 V and varies in a wide range [6], [7].

Manuscript received July 25, 2017; revised September 5, 2017; accepted October 1, 2017. Date of publication October 10, 2017; date of current version February 1, 2018. This work was supported in part by the National Natural Science Foundation of China under Grant 51607113, and in part by the Shanghai Sailing Program under Grant 16YF1407600. Recommended for publication by Associate Editor H. Chung. *(Corresponding author: Haoyu Wang.)*

The authors are with the Chinese Academy of Sciences, Shanghai Institute of Microsystem and Information Technology, University of Chinese Academy of Sciences, Shanghai 200050, China, and also with the Laboratory of Power Electronics and Renewable energies Laboratory, ShanghaiTech University, Shanghai 201210, China (e-mail: shangming@shanghaitech.edu.cn; wanghy.shanghaitech@gmail.com; caoqi@shanghaitech.edu.cn).

Color versions of one or more of the figures in this letter are available online at http://ieeexplore.ieee.org.

Digital Object Identifier 10.1109/TPEL.2017.2761847

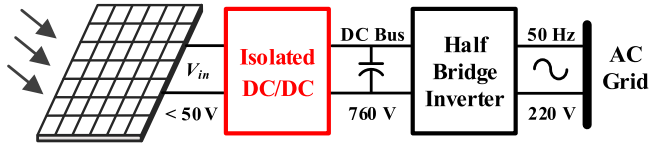

Fig. 1. Structure of a 760 V bus-based two-stage microinverter.

In the front-end dc/dc stage, LLC topology widely attracts researchers' attention due to its high efficiency and intrinsic galvanic isolation [8]. However, it is difficult to realize both overall high efficiency and wide input range simultaneously, since the LLC converter could only maintain high efficiency around resonant frequency [9]. Moreover, to realize the high voltage gain of the LLC converter, the traditional method is to simply increase the turns ratio of the transformer. Nonetheless, high turns ratio results in a large leakage inductance at the higher turns end, and the size and manufacturing cost are increased [10], [11].

To overcome the flaws of the traditional LLC converter, various topologies are proposed. In [12], a modified LLC resonant converter with two transformers is proposed to realize both high efficiency and wide input voltage regulation by changing equivalent magnetizing inductance and turns ratio. However, the increased number of transformers lowers the power density, and the procedure of parameter design is much more complicated than that of a conventional LLC converter. A dual-bridge LLC resonant converter with two operating modes is proposed in [13]. It utilizes the pulse width modulation control at fixed operating frequency for wide input voltage application. In [14], another topology based on the LLC converter with novel frequency adaptive phase shift modulation is proposed to extend its input voltage range. However, none of these topologies is an optimal choice for the front-end stage of 760 V dc bus-based PV microinverters. This is because with those topologies (a) the high voltage gain requires a large transformer turns ratio, and (b) the voltage stresses on the secondary diodes are high and equal to the dc bus voltage.

In order to realize a high voltage gain, a voltage quadrupler rectifier (VQR) based on the traditional LLC converter is utilized in [3], [11]. However, for wide input range applications, the switching frequency window is too wide to maintain high overall efficiency performance.

See http://www.ieee.org/publications_standards/publications/rights/index.html for more information.

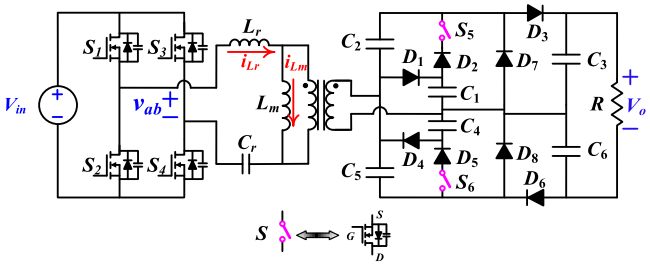

Fig. 2. Schematic of the proposed converter.

To overcome the aforementioned design challenges for LLC topology in microinverter applications, this letter proposes a novel reconfigurable voltage multiplier rectifier for the LLC converter (see Fig. 2). Its rectifier automatically switches among type-4, type-5, and type-6 voltage multiplier configurations, depending on different input voltages. Thus, the switching frequency range can be effectively squeezed and the efficiency over wide input range can be enhanced. This proposed converter demonstrates benefits including (a) soft switching among all power devices, (b) high dc gain with a moderate transformer turns ratio, (c) squeezed frequency modulation range and enhanced overall efficiency, and (d) reduced voltage stresses on the secondary side diodes.

II. Proposed Converter

A. Topology Description

As shown in Fig. 2, the primary side structure of this topology is identical to that of the conventional full-bridge LLC resonant converter. The secondary side is composed of two MOSFETs, eight diodes, and six capacitors. The derivation of this structure is realized by combining a conventional symmetrical VQR with a symmetrical voltage sixfolder rectifier (VSR). This combination is facilitated by adding two MOSFETs, and the novel VSR circuit is proposed by simply extending the VQR converter. Thus, the proposed converter is more suitable for high output voltage applications.

B. Operation Principle

V_2 is the voltage across the capacitor C_2, and V_4 is the voltage across the capacitor C_4.

In order to achieve the desired dc gain range, the proposed topology offers three reconfigurable operation modes illustrated as follows.

Type-4 mode: As shown in Fig. 3(a), diodes $D_{1,2,4,5}$ and capacitors $C_{1,4}$ are disabled by turning OFF the MOSFETs S_5 and S_6. In this case, the circuit operates as conventional VQR configuration, the output voltage is four times of the conventional full-bridge voltage rectifier.

Type-5 mode: As shown in Fig. 3(b), diodes $D_{1,2,8}$ and capacitor C_1 are disabled by just turning ON the MOSFET S_6. In this condition, $V_2 = V_4$, the output voltage is five times of the conventional full-bridge voltage rectifier.

Type-6 mode: As shown in Fig. 3(c), diodes D_7 and D_8 are disabled by turning ON the MOSFETs S_5 and S_6. In this case, $V_2 = 2V_4$, the output voltage is six times of the conventional full-bridge voltage rectifier. Thus, all these operation modes help to reduce the turns of the secondary winding and decrease the parasitic parameters of the transformer.

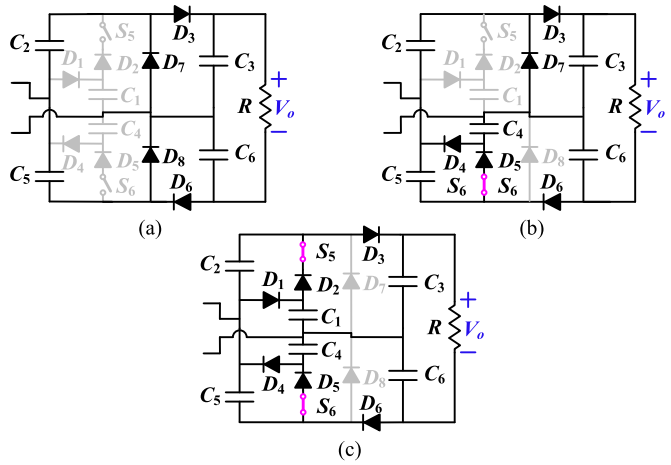

Fig. 3. Converter equivalent circuit configurations: (a) type-4 mode, (b) type-5 mode, and (c) type-6 mode.

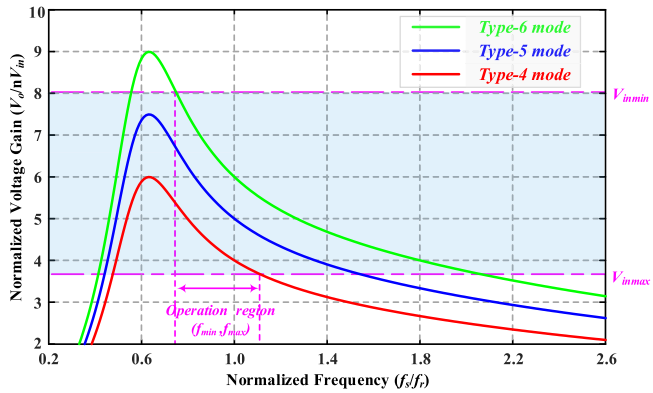

Fig. 4. Normalized voltage gain versus normalized frequency.

C. Voltage Gain

According to the volt-second balance principle of the transformer, V_o can be derived as

$$V_o = \begin{cases} 4V_2, \text{ Type}-4 \text{ mode} \\ 5V_4, \text{ Type}-5 \text{ mode} \\ 6V_4, \text{ Type}-6 \text{ mode} \end{cases}. \quad (1)$$

It should be noted that the voltage applied on the secondary side of the transformer is either V_4 or V_2. Thus, the normalized voltage gain of the proposed converter is defined as

$$G_v = \frac{V_o}{nV_{\text{in}}} = \begin{cases} \frac{4V_2}{nV_{\text{in}}}, \text{ Type}-4 \text{ mode} \\ \frac{5V_4}{nV_{\text{in}}}, \text{ Type}-5 \text{ mode} \\ \frac{6V_4}{nV_{\text{in}}}, \text{ Type}-6 \text{ mode} \end{cases}. \quad (2)$$

The normalized gain curves of the converter are plotted in Fig. 4. As shown, a wide voltage gain range with a

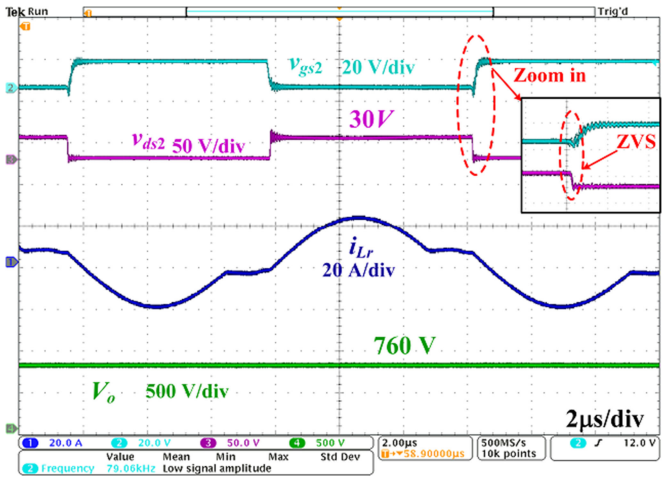

Fig. 5. Steady-state waveforms in type-6 mode.

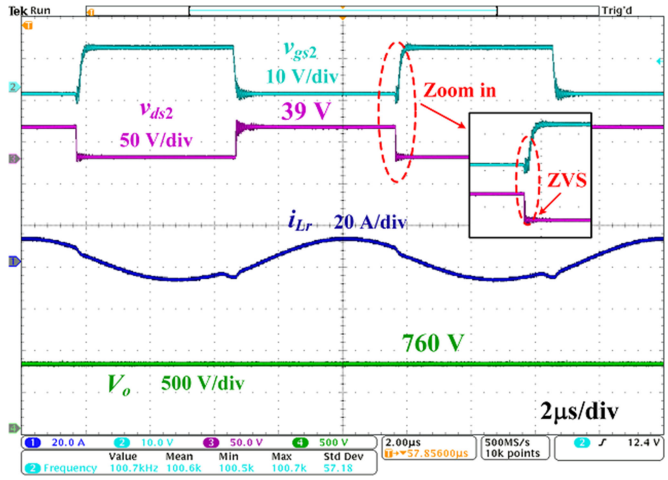

Fig. 6. Steady-state waveforms in type-5 mode.

comparatively narrow switching frequency range can be achieved by adaptively changing the converter operation mode.

III. Experimental Results

A 300 W experimental prototype for PV microinverters application is built to verify the effectiveness of the proposed LLC resonant converter. A solar array simulator (Chroma 62020H-150S) is used to emulate the output of the solar panel. The specifications and design parameters are listed as follows. $V_{\text{in}} = 25 - 50\,\text{V}$, $V_o = 760\,\text{V}$, $S_1 - S_4$: IRFP3306, S_5 and S_6: STW88N65M5, $D_1 - D_6$:C3D04060A, transformer's turns ratio $n = N_P$: $N_S = 10:40$, $L_m = 13\,\mu\text{H}$, $L_r = 4.1\,\mu\text{H}$, $C_r = 620\,\text{nF}$, the resonant frequency $f_r = 100\,\text{kHz}$, and the switching frequency range is within 75–110 kHz.

The steady-state waveforms of the proposed LLC converter in type-6 mode with $V_{\text{in}} = 30\,\text{V}$ and $V_o = 760\,\text{V}$ are shown in Fig. 5. It can be seen that v_{ds2} drops to zero before gate signals are applied to the MOSFETs. Therefore, ZVS is achieved on S_2. At this operating point, the waveform of i_{Lr} shows that f_s is lower than f_r.

The steady-state waveforms of the converter operating in type-5 and type-4 modes with inputs of 39 V and 50 V are captured in Figs. 6–8. It can be considered as the sign of ZVS among all primary side MOSFETs. Moreover, the diode current waveform is captured in Fig. 7. It shows that the diode is turned OFF with zero current. Therefore, the diode reverse recovery process is eliminated.

To achieve a good dynamic response, two feedback control loops must be enforced. The outer loop controls the mode transition based on different input voltage ranges, whereas the inner loop implements the frequency modulation based on PI compensation. A TMS320F28335 Digital Signal Processor (DSP) from Texas Instruments is used to implement the digital control algorithm.

Figs. 9 and 10 show the mode transition waveforms. The threshold voltages are set to be 36 V and 44 V, respectively. As shown in Fig. 9, when the input voltage is lower than 36 V, the converter will operate in type-6 multiplier mode, meanwhile,

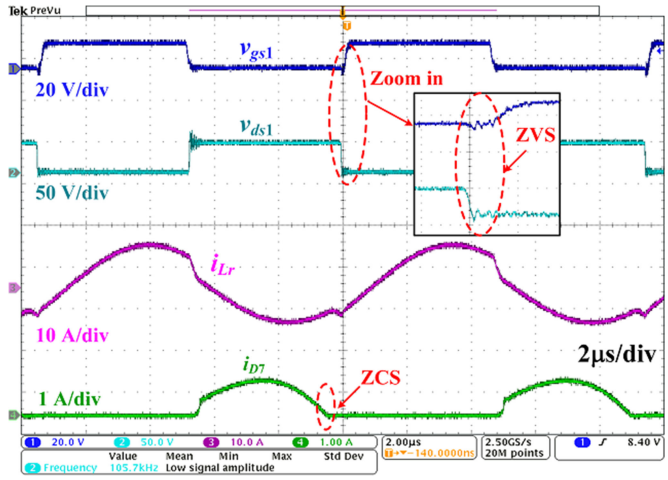

Fig. 7. ZVS and ZCS waveforms in type-5 mode.

$S_{5,6}$ are always ON. When the input voltage is larger than 36 V and lower than 44 V, S_5 will turn OFF and then the converter will operate in type-5 multiplier mode. When the input voltage is larger than 44 V, S_6 will turn OFF and then the converter will operate in type-4 multiplier mode. Under the same condition above, the waveform of i_{Lr} is shown in Fig. 10. As shown in Figs. 9 and 10, it can be seen that the smooth mode transition is achieved and the output voltage is controlled to be 760 V when the input voltage increases.

Practically, the input voltage changes slower than the step changes demonstrated in Fig. 9. The experiment with a gradually changing V_{in} is conducted and the corresponding waveforms are captured in Fig. 11. The output voltage disturbance is constrained to be 6.5%, which is considered as acceptable.

Fig. 12 shows the curves of efficiency versus input voltage of the designed prototype with constant input current 6 A. At 36 V input voltage, type-5 mode demonstrates slightly higher efficiency than type-6 mode, and higher efficiency can be achieved in type-4 mode when the input voltage is higher than 44 V. Therefore, 36 V and 44 V are selected as the threshold voltages to trigger the configuration switches. Meanwhile, it can

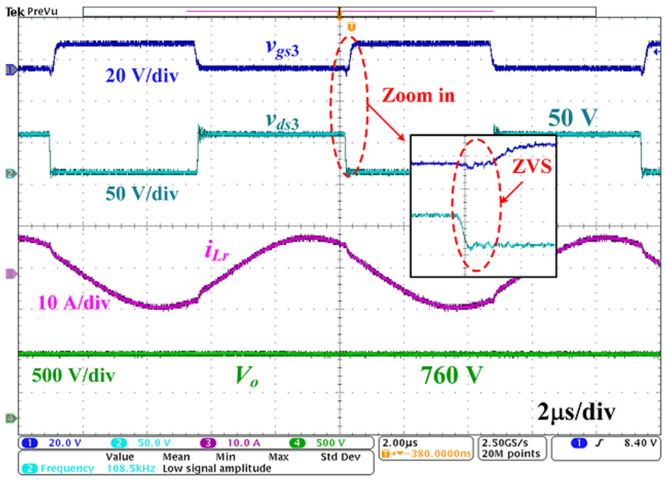

Fig. 8. Steady-state waveforms in type-4 mode.

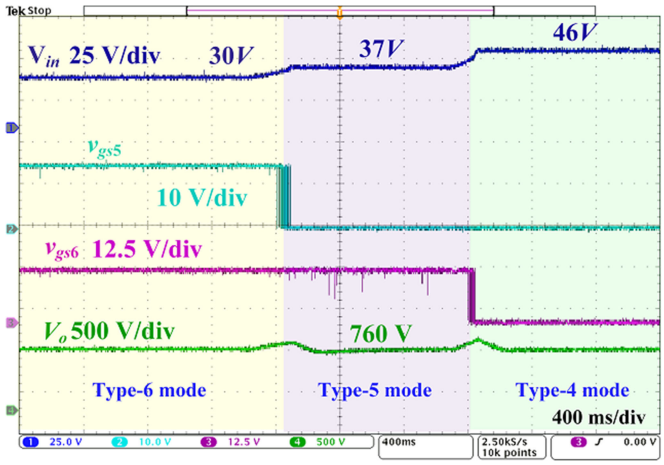

Fig. 9. Experimental voltage waveforms of mode transition.

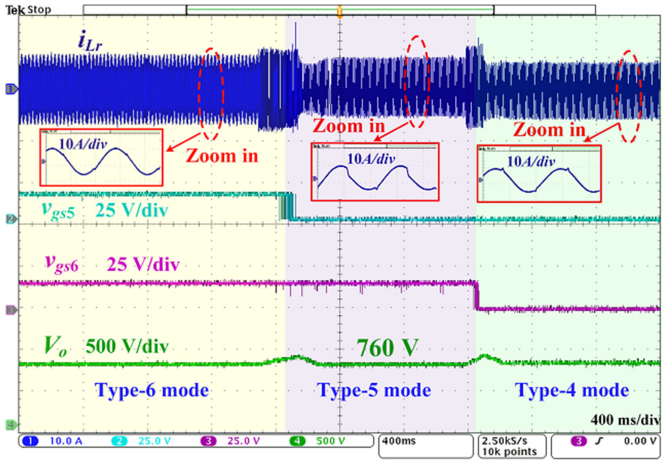

Fig. 10. Experimental current waveforms of mode transition.

be seen that the measured efficiency of the conventional LLC resonant converter with VQR is lower than that of the proposed converter.

Figs. 13–15 show the curves of measured efficiency versus input power under different input voltages. It should be noted that

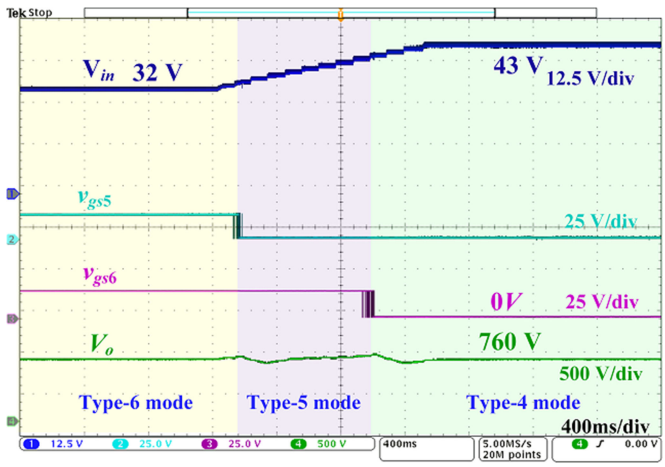

Fig. 11. Experimental waveforms of the mode transition with a slow change of V_{in}.

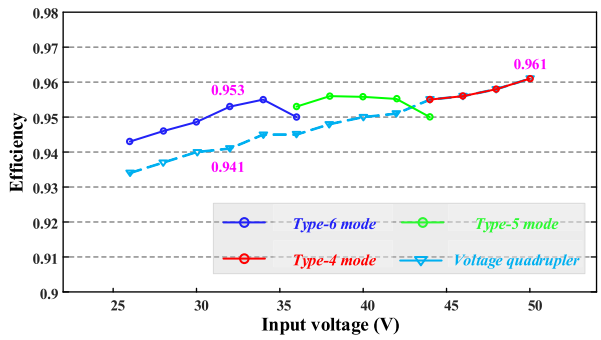

Fig. 12. Measured converter efficiency versus input voltages with $I_{\text{in}} = 6$ A.

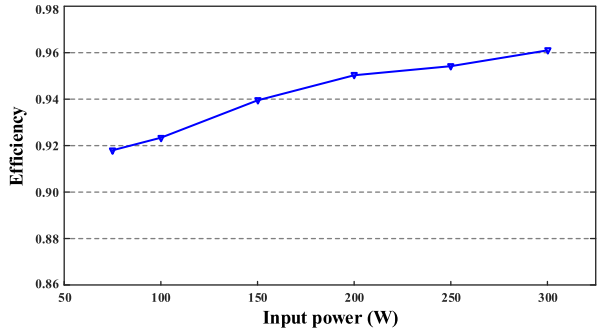

Fig. 13. Measured efficiency versus input power with $V_{\text{in}} = 50$ V.

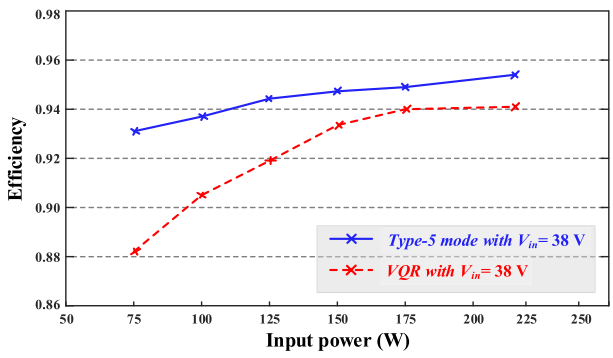

Fig. 14. Measured efficiency versus input power with $V_{\text{in}} = 38$ V.

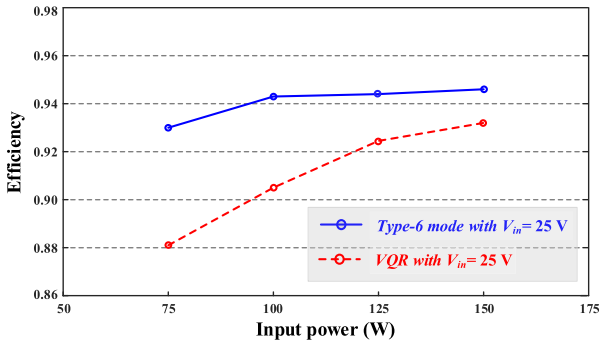

Fig. 15. Measured efficiency versus input power with $V_{\text{in}} = 25$ V.

with $V_{\text{in}} = 25$ V, the efficiency curve of VQR LLC converter overlaps with the type-4 mode of the proposed reconfigurable converter. As shown in Figs. 14 and 15, when the input voltage deviates from 50 V, the proposed reconfigurable converter demonstrates obviously higher conversion efficiency than the conventional VQR converter over a wide power range. This is mainly due to the fact that proposed reconfigurable converter owns the benefit of the squeezed frequency range and reduced power losses.

IV. Conclusion

In this letter, a novel self-reconfigurable LLC type resonant topology is proposed. The circuit operation principles are analyzed. The converter can operate at a narrow switching frequency range by dynamically configuring the operation mode of the rectifier. Thus, in comparison with conventional LLC resonant converter with a full-bridge rectifier, the proposed converter is more suitable for wide input range and high output voltage applications. A 300 W prototype with 25–50 V input voltage and 760 V output voltage is designed to verify the circuit functionality. The proposed topology is not only useful for PV microinverter applications, but also worthy of pursuing in applications where a wide voltage gain range and a high output voltage are desired.

References

[1] L. Chen, C. Hu, Q. Zhang, K. Zhang, and I. Batarseh, "Modeling and triple-loop control of ZVS grid-connected DC/AC converters for three-phase balanced microinverter application," *IEEE Trans. Power Electron.*, vol. 30, no. 4, pp. 2010–2023, Apr. 2015.

[2] X. Zhao, L. Zhang, R. Born, and J. -S. Lai, "A high-efficiency hybrid resonant converter with wide-input regulation for photovoltaic applications," *IEEE Trans. Ind. Electron.*, vol. 64, no. 5, pp. 3684–3695, May 2017.

[3] Y. Zhao, X. Xiang, W. Li, X. He, and C. Xia, "Advanced symmetrical voltage quadrupler rectifiers for high step-up and high output-voltage converters," *IEEE Trans. Power Electron.*, vol. 28, no. 4, pp. 1622–1631, Apr. 2013.

[4] H. Hu, S. Harb, N. Kutkut, I. Batarseh, and Z. J. Shen, "A review of power decoupling techniques for microinverters with three different decoupling capacitor locations in PV systems," *IEEE Trans. Power Electron.*, vol. 28, no. 6, pp. 2711–2726, Jun. 2013.

[5] S.-M. Chen, T.-J. Liang, L.-S. Yang, and J.-F. Chen, "A safety enhanced, high step-up DC–DC converter for AC photovoltaic module application," *IEEE Trans. Power Electron.*, vol. 27, no. 4, pp. 1809–1817, Apr. 2012.

[6] D. Meneses, F. Blaabjerg, O. García, and J. A. Cobos, "Review and comparison of step-up transformerless topologies for photovoltaic AC-module application," *IEEE Trans. Power Electron.*, vol. 28, no. 6, pp. 2649–2663, Jun. 2013.

[7] B. Liu, S. Duan, and T. Cai, "Photovoltaic DC-building-module-based BIPV system—Concept and design considerations," *IEEE Trans. Power Electron.*, vol. 26, no. 5, pp. 1418–1429, May 2011.

[8] H. Wang, S. Dusmez, and A. Khaligh, "Design and analysis of a full bridge LLC based PEV charger optimized for wide battery voltage range," *IEEE Trans. Veh. Technol.*, vol. 63, no. 4, pp. 1603–1613, Apr. 2014.

[9] H. Wang and Z. Li, "A PWM LLC type resonant converter adapted to wide output range in PEV charging applications," *IEEE Trans. Power Electron.*, to be published.

[10] P. Saadat and K. Abbaszadeh, "A single-switch high step-Up DC–DC converter based on quadratic boost," *IEEE Trans. Ind. Electron.*, vol. 63, no. 12, pp. 7733–7742, Dec. 2016.

[11] A. K. Singh, P. Das, and S. K. Panda, "Analysis and design of SQR-based high-voltage LLC resonant DC–DC converter," *IEEE Trans. Power Electron.*, vol. 32, no. 6, pp. 4466–4481, Jun. 2017.

[12] H. Hu, X. Fang, F. Chen, Z. J. Shen, and I. Batarseh, "A modified high-efficiency LLC converter with two transformers for wide input-voltage range applications," *IEEE Trans. Power Electron.*, vol. 28, no. 4, pp. 1946–1960, Apr. 2013.

[13] X. Sun, X. Li, Y. Shen, B. Wang, and X. Guo, "Dual-bridge LLC resonant converter with fixed-frequency PWM control for wide input applications," *IEEE Trans. Power Electron.*, vol. 32, no. 1, pp. 69–80, Jan. 2017.

[14] S. M. S. I. Shakib and S. Mekhilef, "A frequency adaptive phase shift modulation control based LLC series resonant converter for wide input voltage applications," *IEEE Trans. Power Electron.*, vol. 32, no. 11, pp. 8360–8370, Nov. 2017.